Tellus A
Dynamic Meteorology and Oceanography

A Simple Model for an Internal Wave Spectrum Dominated by Non-Linear Interactions

ORIGINAL RESEARCH PAPER

HANS VAN HAREN
LEO MAAS
*Author affiliations can be found in the back matter of this article

STOCKHOLM UNIVERSITY PRESS

ABSTRACT

Ocean motions at frequencies of the internal wave band are generally associated with freely propagating waves that are supported by stable vertical stratification in density. Previous analyses of yearlong current observations from the Bay of Biscay showed that a finestructure of semidiurnal tidal and near-inertial higher harmonics fills the spectrum. Here, a simple model is presented of forced nondispersive motions with forward energy cascade. The model fits the spectral shape of higher harmonics well within statistical significance and shows that such interactions imply maximum wave steepness in a balance between forcing and turbulent mixing. The single fitting parameter takes a value of approximately one, at which the barotropic tidal flow speed equals the internal wave phase speed. We infer that the barotropic tide sets a non-linear limit to baroclinic current scales without generating non-linear higher harmonics directly.

CORRESPONDING AUTHOR:

Hans van Haren

Royal Netherlands Institute for Sea Research (NIOZ), P.O. Box 59, 1790 AB Den Burg, the Netherlands

hans.van.haren@nioz.nl

KEYWORDS:

internal wave observations; Bay of Biscay; non-linear higher harmonics; advection model; forward cascade

TO CITE THIS ARTICLE:

van Haren, H and Maas, L. 2022. A Simple Model for an Internal Wave Spectrum Dominated by Non-Linear Interactions. *Tellus A: Dynamic Meteorology and Oceanography*, 74(1): 382–390. DOI: https://doi.org/10.16993/tellusa.45

1. INTRODUCTION

Following in situ observations (e.g., Pinkel et al., 1987; Mihaly et al., 1998; van Haren et al., 1999) and numerical modeling (e.g., Xing and Davies, 2002; Pichon et al., 2013) the oceanic internal wave 'IW' band is not always a smooth broadband spectrum, but it can be dominated by a sequence of peaks associated with near-inertial and/or semidiurnal tidal motions and their higher harmonics.

In theory, freely propagating internal gravity waves can exist in the IW frequency (σ) band between $|f(\varphi)| < \sigma < N(z)$, $N >> f$. The frequency range is limited at the high end by the depth (-z) dependent buoyancy frequency $N(z) = (-g(d\ln\rho/dz+g/c_s^2))^{1/2}$, where g is the acceleration of gravity, and c_s the speed of sound describing compressibility effects. At the low end, it is limited by the latitudinal (φ) dependent inertial frequency $f(\varphi) = 2\Omega\sin\varphi$, which is twice the local vertical component of the Earth's rotation vector Ω (e.g., LeBlond and Mysak, 1978). Suggestions have been made (Mihaly et al., 1999; Xing and Davies, 2002) that near-inertial motions are important for transfer of energy inside the IW-band through non-linear interaction with semidiurnal tidal motions. Higher tidal and inertial-tidal harmonics are not only observed in shallow seas (van Haren et al., 1999), but also in the deep ocean near and away from topography (Mihaly et al., 1998; van Haren et al., 2002). These observations seemed to confirm the hypothesis that (breaking) non-linear internal waves may be important for diapycnal mixing (Müller and Briscoe, 1999).

In this paper a simple heuristic model is proposed describing non-linear interactions that generate such higher harmonics peaks in the IW-band and fit the spectral shape of yearlong current meter observations from the deep Bay of Biscay. The model follows theoretical suggestions (Phillips, 1977) on forced non-resonant interactions and adds to continuous smooth spectra (Garrett and Munk, 1972) describing a symmetric and isotropic linear wave field without tides. By investigating tidal and inertial-tidal higher harmonics, it differs from open-ocean models describing weakly non-linear resonant and near-resonant interactions that lack motions at these frequencies (e.g., McComas and Bretherton, 1977; Lvov et al., 2012; Eden et al., 2019). Previously, no model existed for the spectral shape of non-linear higher harmonics in the open-ocean, although there were studies about relative importance of such constituents in tidal context, mainly for shallow seas (Dronkers, 1964; Pingree and Maddock, 1978; Parker, 1991). Hence, their naming as 'shallow water—tidal—constituents', which are for instance important for frictionally induced sediment transport (Groen, 1967). Because non-linear friction is considered small in the open-ocean, we here consider non-linear advection, which occurs in the momentum equations, to describe deep-ocean motions at higher harmonic interaction frequencies.

It is common that simplified models are based on strong assumptions. The simplified 'cartoon' model, proposed below, describes the cascade of tidal and inertial-tidal higher harmonics. It not only assumes that advection dominates other forces in the equation of motion, but also that advection of the 'barotropic' surface tide as well as of inertial motions does not play a role due to large scales compared to the small scale of the internal-tide. This scale-separation immediately clarifies why inertial-inertial interactions, leading to motions at frequencies 2f, 3f etc., and, consequently, advection of the 'baroclinic' internal tide by these inertial higher harmonics, that would e.g. lead to M_2+2f, are weak. M_2 denotes the semidiurnal lunar tidal frequency.

Uniformly-stratified fluids may display both free, resonant as well as forced, non-resonant higher harmonics (Phillips 1977). These forced higher harmonics do not obey the free-wave dispersion relation. As shown here, such harmonics as observed in the deep Bay of Biscay, can apparently be captured by a simple one-parameter recursive non-linear model. Interestingly, the estimated value of the single fitting parameter suggests this occurs when the barotropic current approximately equals the internal wave phase speed.

2. OBSERVATIONS

Currents were evaluated from two moorings deployed in the Bay of Biscay NE-Atlantic Ocean during 11 months, above the continental slope at 46°39´ N, 05°29´ W (water depth H = 2450 m) and above the abyssal plain at 45°48´ N, 06°50´ W (H = 4810 m), see Figure 1. The focus is on data from the uppermost Aanderaa RCM-8 single-point current meter at 1000 m above the bottom in each mooring. This distance above the seafloor is well above any internal wave breaking at the local seafloor slope. Horizontally, it is at least 10 km from topography, and the deepest site is more than 100 km from the foot of the continental slope. However, the rugged continental slope shows strongly non-linear internal waves that vigorously break (e.g., van Haren, 2006). The continental slope is also where internal (tidal) waves are generated and where these waves possibly are focused by reflection. It is unknown however, how far from the slope its effects are sensed. Numerical modelling suggests the spread of internal tides throughout the Bay of Biscay (e.g., Pichon et al., 2013).

From a few CTD density profiles, obtained near the moorings, stratification was estimated $N(z) = (1 \pm 0.5)(20 + 0.0034z)$ cpd, $-4480 < z < -2740$ m (frequency was calculated in cycles per day, 1 cpd = $2\pi/86400$ s^{-1}). The

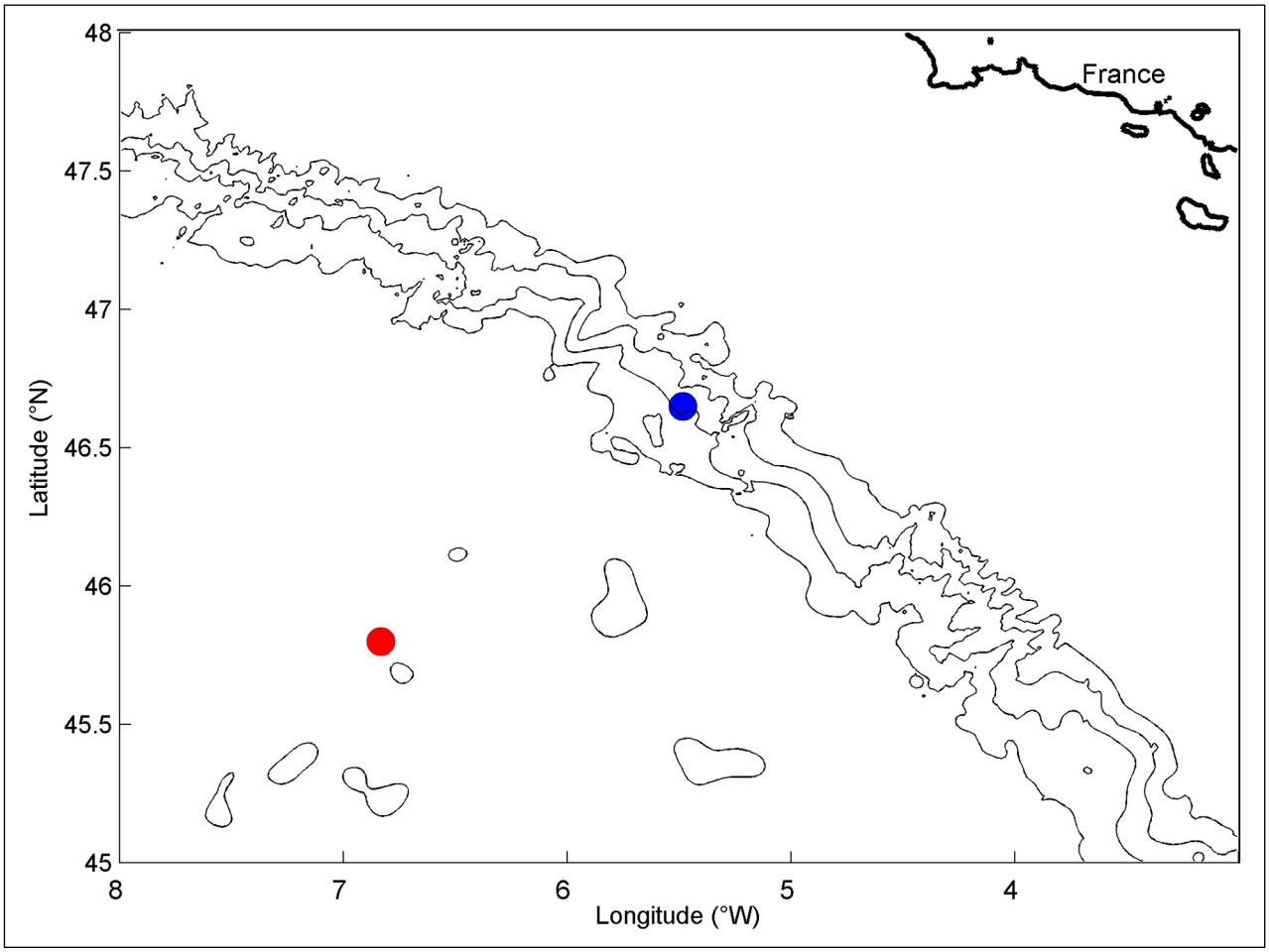

Figure 1 Current meter mooring sites in the Bay of Biscay with black contours of topography every 1000 m water depth. The coloured dots correspond with the spectra in Figure 2.

significant one-standard deviation of variations follows from computations over small 10-m vertical scales that will play a significant role in the modelling later on. The large-scale depth dependence changed abruptly above 2740 m. At 1500 m, N ≈ 28 cpd.

Tidal harmonic analysis (Dronkers, 1964) was used to split a highly deterministic narrowband large-scale signal, here termed 'barotropic' signal, from the remainder 'baroclinic' or internal, difference signal. The application of the sharp harmonic band-pass filter to the 11-month long records results in a small fundamental bandwidth which is more than an order of magnitude smaller than the bandwidth of baroclinic signals and ensures an effective split (van Haren, 2016). Because we use current meters, the barotropic signal represents a time-coherent signal at a limited number of semidiurnal constituents. At M_2 the barotropic signal is about twice the value of the baroclinic signal.

Observed kinetic energy spectra $P_{KE}(\sigma)$ revealed larger energy at shallower depth (where N is larger), except at f (Figure 2). For the entire IW-band larger energy was found at localized frequencies associated with inertial and semidiurnal tidal motions (indicated as f and (lunar) M_2, respectively) and higher harmonics (indicated as M_4, M_6,...and M_2+f, M_4+f...). These energy peaks exceeded the spectral continuum that sloped with frequency like $P_{KE} \sim \sigma^{-1}$, for $f < \sigma < 7$ to 10 cpd. A σ^{-1} spectral slope, 'pink noise' (Schroeder, 1991), has been observed in temperature spectra from other open-ocean areas away from topography (van Haren and Gostiaux, 2009). Such a σ^{-1} spectrum is broadly seen as bearing evidence of self-organized criticality (Bak et al., 1987), the generation of barely stable structures of critical states (Schroeder, 1991). It motivates this paper's interpretation of observed tidal and inertial-tidal harmonics as bearing evidence of a fast and non-linear IW-interaction up to the point of breaking. At higher frequencies, the continuum sloped steeper. Higher harmonics were observed above their respective continuum levels up to M_{10} at the deeper site and up to M_{16} at the shallower site. The higher harmonics were found in a sequence of decreasing amplitudes. Recalling that the observations were made at single points in space, it is unlikely that they represent locally-forced, freely-propagating higher harmonic internal waves (e.g., Lamb, 2004). At different internal wave frequencies, energy would propagate along differently inclined beams, which would not provide a monotonically decreasing sequence of higher harmonics

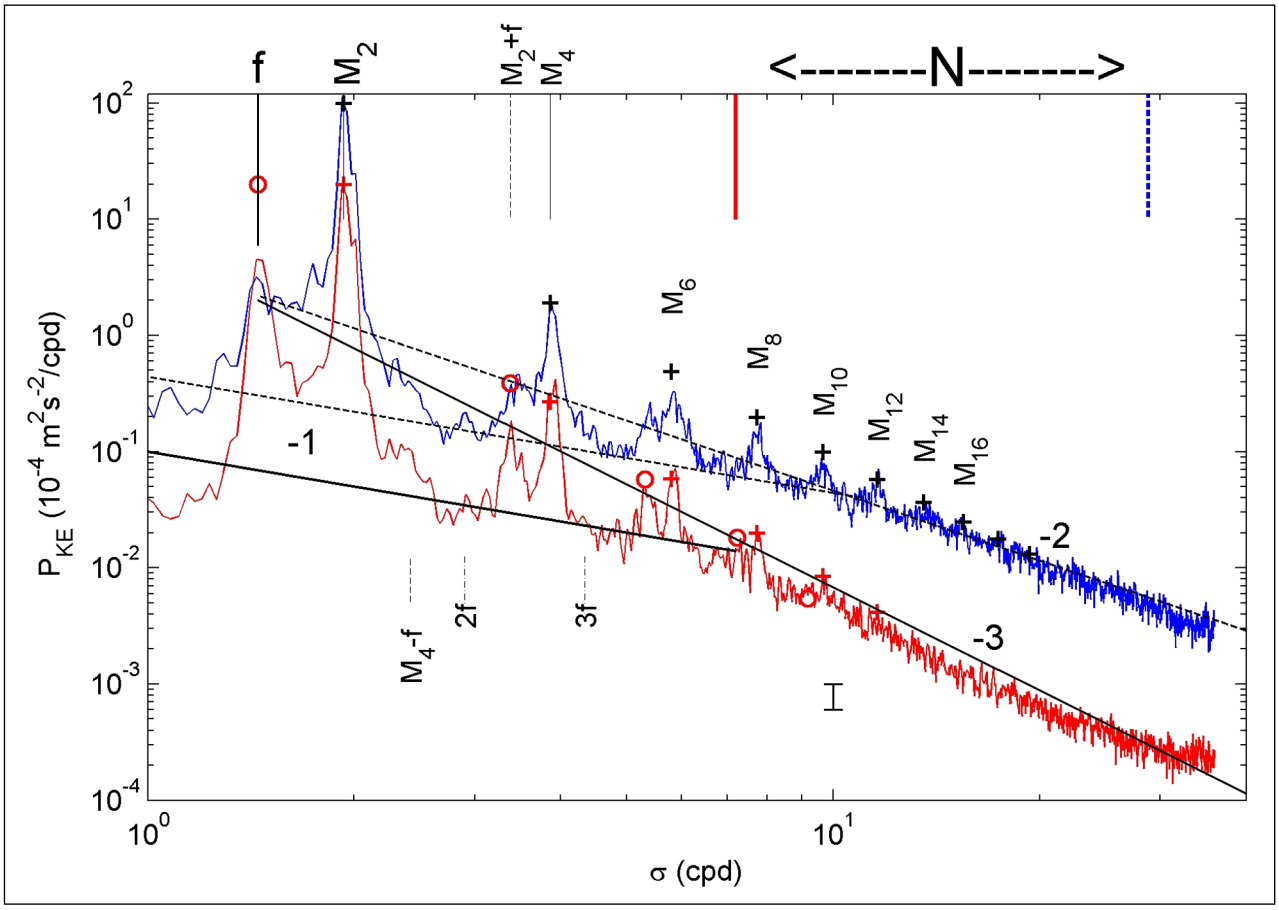

Figure 2 Kinetic energy spectra from 11 months of current meter observations at 1000 m above the seafloor in H = 4810 m water depth (red) and H = 2450 m (blue). Spectra were moderately smoothed (ν ≈ 30 df) and not offset vertically. The difference in energy levels between the spectra corresponded to the difference in N(z), which variation is indicated between the vertical bars in the top-right corner. This corresponds with the vertical distance between the sloping lines at fall-off rates σ^{-1} (solid and dashed corresponding to red and blue spectra, respectively). Constant slopes in log-log plot are indicated "–1,–2,–3" representing σ^{-1}, σ^{-2}, σ^{-3}, respectively. Spectra of model (2) are superposed for observed barotropic and baroclinic fundamental tidal amplitudes and fitting parameter γ. Three model examples are given, two for tidal-interactions (+) and one for inertial-tidal-interactions including frequency-corrections to coefficients (o). They fit well the observed energy levels for nearly the same γ (see text). In all cases, reference amplitude is the barotropic M_2 current amplitude, indicated at f and M_2 (leftmost o, +). Baroclinic M_2-variance are a quarter of peak M_2-values.

variance in single-point measurements as observed here (but possibly only when averaged over many spatially distributed instruments).

When the kinetic energy was large at f (deepest mooring, small N), energy at f-interaction frequencies (e.g. M_2+f) showed a spectral fall-off rate with frequency like $P_{KE} \sim \sigma^{-3}$, which was a typical fall-off rate, or even steeper, for higher tidal harmonics, see red plusses in Figure 2. When energy at f was reduced (shallowest mooring, large N), energy at M_n+f, n = 2, 4,..., scaled like $\sim\sigma^{-2}$. When smoothed strongly, the latter records showed overall spectral fall-off rate close to $\sim\sigma^{-2}$ for f < σ < N (van Haren et al., 2002). For the deepest mooring with relatively large inertial-tidal and tidal harmonics, the heavily smoothed overall spectral fall-off rate was faster $\sim\sigma^{-3}$. This is significantly steeper than the canonical fall-off rate $P_{KE} \sim \sigma^{p}$, –2.5 < p < –1.5 for open-ocean internal waves (Garrett and Munk, 1972). At 2f, 3f, M_2+2f, etc., motions do not exceed the continuum level (van Haren et al., 2002), a property we commented on in Section 1.

3. SPECTRAL MODEL FOR INTERNAL WAVE HIGHER HARMONICS

In an inviscid uniformly-stratified fluid, a single-frequency free plane obliquely propagating internal wave (or a set of collinear propagating plane waves) is governed by linear equations as the non-linear advection terms exactly cancel in the equations for vorticity and buoyancy (LeBlond and Mysak, 1978). This follows from the absence of variations in the planes of equal phase, and which distinguishes internal from surface waves. In a tilted (ξ, ζ)-frame (Figure 3a), a plane internal gravity wave (wave vector $\mathbf{k}$ = (k, l) = (0, l)) has its velocity vector $\mathbf{u}$ = (û, ŵ) = (û, 0) perpendicular to the ζ-direction into which velocity and buoyancy perturbations vary. This follows from incompressibility, $\nabla\cdot\mathbf{u} = 0$, which implies $\mathbf{k}\cdot\mathbf{u} = \mathbf{u}\cdot\mathbf{k} = 0$, meaning that also the advection operator vanishes, $\mathbf{u}\cdot\nabla = 0$.

However, in reality non-linearity is not expected to vanish. Like surface waves, internal waves may manifest themselves partially as displacement waves on layers

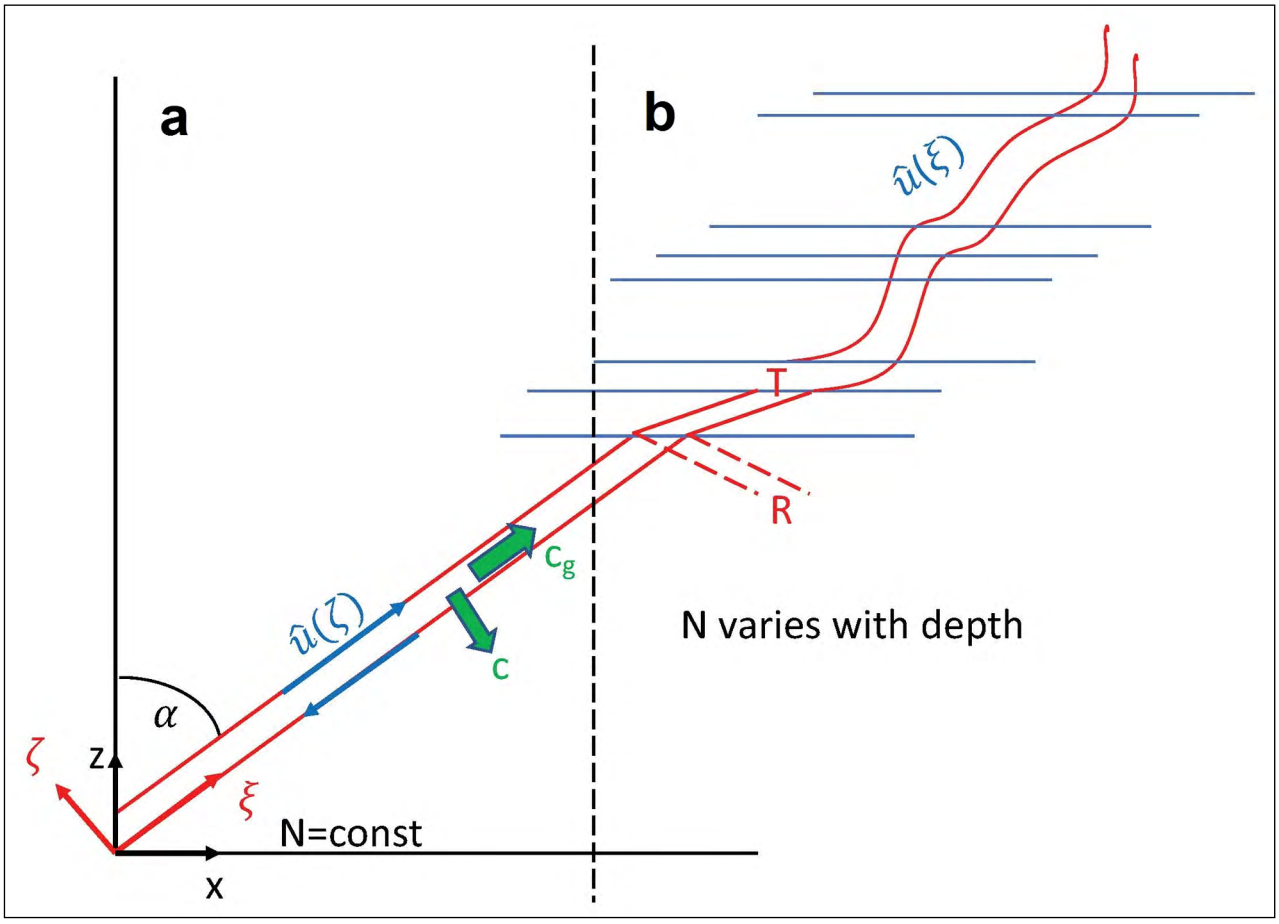

Figure 3 Sketch of internal tidal velocity and its direction of variation. **(a)** In a uniformly stratified ocean velocity only varies in the direction of phase speed c, not in the direction of energy propagation c_g. **(b)** In a non-uniformly stratified ocean in which incoming energy splits in transmitted (T) and reflected parts (R) velocity may vary dominantly in the direction of energy propagation when the scale of variation in ξ is smaller than the wavelength of the incident internal wave. The blue lines indicate isopcynals whose smaller distance between them implies stronger stratification across an interface.

of enhanced stratification. This is because the ocean rather consists of non-uniform, alternatingly weaker and stronger stratified layers (interfaces) (Figure 3b). Such 'interface waves' may grow up to highly non-linear shock waves (Platzman, 1964). Due to variations in source, for example at different sites and due to varying stratification, internal waves propagate in groups of limited size which provides their intermittent character, and non-linearity may be imperative to prevent dispersion (Thorpe, 1999).

Sofar, no general solution has been given to describe strongly non-linear internal wave motions using the full set of governing equations (Shrira, 1981). The mathematics is too complex. Theoretical and numerical modelling has been performed on weakly non-linear interactions between open-ocean internal waves and in idealized settings under resonant or near-resonant conditions (e.g., McComas and Bretherton, 1977; Lvov et al., 2012; Eden et al., 2019). The ocean models find low and high frequency energy representing currents and waves, leaving a gap between 2f and 3f, But such energy gap is not generally found in ocean observations. Idealized tidal models under near-resonant conditions typically consider incident, horizontally-propagating, vertically-standing internal modes (Baker and Sutherland, 2020), or internal wave beams obliquely incident on vertically rapidly varying 'thin-layer' stratification (Diamessis et al., 2014). Such models do find (first) higher harmonics, but only near the main pycnocline and not throughout the deep ocean.

However, considering that internal waves occur intermittently (Wunsch, 1975) and in groups, we infer that the occurrence of rapid variations in stratification on scales much smaller than the internal wavelength must be ubiquitous. This prohibits an innocuous adiabatic (WKB) adjustment of a passing internal wave beam. Instead, it gives rise to its genuine scattering, which continuously involves the partial reflection of the principal internal wave beam. This implies that now some transverse motion occurs all along the incident wave beam, reinvigorating the non-linear advection. The crude way in which we aim to take this into account in our simple model is to acknowledge that along-beam velocity variations now occur on very small scales all along the internal wave beam. This simple model, along the lines of non-linear wave deformation found in shock waves (Platzman, 1964), is adopted here as it adequately predicts an energy spectrum of higher harmonics, as observed.

Consider a deformed wave's discrete kinetic energy spectrum $P_j(\sigma_j) = \frac{1}{2}\hat{U}_j\hat{U}_j^*$, the asterisk denoting complex conjugate, of IW scalar current components $\hat{u}_j = \hat{U}_j\exp[i(k_j\xi-\sigma_j t)]$ with frequency σ_j, wavenumber k_j and scalar amplitude $\hat{U}_j$. Here, $i^2 = -1$ and j is a positive integer starting from the fundamental baroclinic component j = 1. The coordinate ξ is in the oblique energy propagation direction of the deformed wave, parallel to the phase lines. It is assumed to indicate the direction of the largest baroclinic current component û, associated with an internal tidal beam, but this beam is deformed by non-uniform stratification (Figure 3b). This lends the beam an along-beam variation at wave number k_1. Compared to the horizontal barotropic current, the latter may have a relatively large component in the perpendicular direction. Similar along-beam variations have been considered in sophisticated models concerned with subharmonic internal wave generation (Fan and Akylas, 2021), absent in our observations.

Remark that the incident internal wave beam ~exp(-*il*ζ) in a uniformly stratified fluid contains the dependence on the transverse ζ-direction, into which its phase mainly propagates (Figure 3a). But in the non-uniformly stratified fluid the wave's cross-beam wavenumber *l* is assumed to be small, $l \ll k_j$. Thus the ζ-dependence is suppressed here (it is assumed to be virtually uniform on the scale of the along-beam variations), and does not contribute non-linearly to the higher harmonics. This leaves the along-beam velocity, or the velocity of interface waves resulting from beam-transmission and –reflection, now having a ξ-dependence due to non-uniform stratification (Figure 3b). This is also affected by the presence of mean-flow shear, and non-Boussinesq and viscous effects. Ocean measurements indeed reveal such variations along the internal tidal beam through patchiness of the along-beam velocity (van Haren et al., 2010) that motivates this description of $\hat{u}_j$.

In our model discrete spectrum only those parts are considered that are entirely governed by advection in the wave-energy propagation direction, ξ, and no advection perpendicular to this direction. The model expresses forced non-linear interactions between linear motions that result in bound non-freely-propagating motions. Rotation is neglected by assuming that interactions are fast compared with the inertial period, resulting in motions at frequencies $\sigma \gg f$. A pressure gradient forcing is assumed being linear and only governing the fundamental (j = 1) tidal component. Diffusion is neglected. For clarity, we here exclude both advection by a barotropic surface tidal current $\hat{u}_0$ ($\hat{U}_0$, $\sigma_0 = \sigma_1$, $k_0 \approx 0$), since we consider motions within a barotropic oscillating system, as well as advection of the barotropic component because its wavenumber $k_0 \ll k_1$. We thus base the following cartoon model (1) on the shock-wave model of Platzman (1964) and on dominance of the advection term describing non-linear motions in shallow seas (Pingree and Maddock, 1978; Xing and Davies, 2002). The model apparently captures our deep-ocean observations for j = 2, 3, ...,

$$\frac{\partial \hat{u}_j}{\partial t} = -\sum_{i=1}^{j-1} \hat{u}_i \frac{\partial \hat{u}_{j-i}}{\partial \xi}. \quad (1)$$

Only non-resonant higher harmonics $\sigma_j = j\sigma$ and $k_j = jk$ are found here as the compound wave's frequency and wavenumber do not themselves satisfy the dispersion relation, required for resonant triads (Dauxois et al., 2018). This means that the newly generated higher harmonics do not propagate as free waves along a different inclination, away from the beam they are generated by. Instead they propagate along the beam, in their turn advecting spatial variations in a like manner along the beam.

Equation (1) implies a forward cascade of energy from a source at a fundamental baroclinic internal (tidal) constituent (σ_1, k_1, $\hat{U}_1$) ≡ (σ, k, Û), determining the amplitudes of the successive harmonics,

$$\hat{U}_j = \left(\frac{k}{\sigma}\right)\sum_{i=1}^{j-1}\frac{j-i}{j}\hat{U}_i\hat{U}_{j-i} \equiv q_j\gamma^{j-1}\hat{U}, \quad (2)$$

recursively defining factors $q_j = \frac{1}{2}, \frac{1}{2}, \frac{5}{8}, \frac{7}{8}, \frac{21}{16}, \ldots$ for j = 2,3,4,5,6, ..., etcetera, and depending only on parameter $\gamma = \hat{U}/c$, with $c = \sigma/k$ denoting the phase-speed of the fundamental harmonic. A constant c ($c_j \equiv \sigma_j/k_j = c$), as found here for all the higher harmonics of the baroclinic M_2 tide, is remarkable. It not only implies non-dispersive wave steepening, but, since the internal wave and its higher harmonics are synchronized a spatio-temporal coherency. As we will see below, this synchronization is lost when waves of other frequencies and wave numbers advect the baroclinic tide. In that case the compound frequency and wave number do no longer grow at the same rate, implying varying c_j and loss of coherency. This translates in an absence of spectral peaks at frequencies as M_2+2f etc. The model (2) contrasts with the shock-wave model by Platzman (1964), which also includes a backward cascade.

From (2) a consistent model spectrum $P_m(\sigma) = \sum_j P_j(\sigma_j)$ is obtained fitting the observed kinetic energy at discrete frequencies $\sum_j P_{df}(\sigma_j)$ after tuning to $\gamma = 0.48 \pm 0.05$ under the conditions $|\log(P_{df}(\sigma_j)/P_j(\sigma_j))| < 10\%$ for all j and $\sigma < N$ (Figure 2). The first condition implies that the observed and modelled spectra do not differ by more than 10% in variance at the discrete interaction frequencies. The small standard deviation, which is well within 95% statistical significance of the spectra, expresses the sensitivity of the model to γ. It yields the surprising result that $\hat{U}_0 = (0.96 \pm 0.11)c$, using observed $\hat{U}_0/\hat{U} = 2.0 \pm 0.15$ following harmonic analysis splitting the original signal into semidiurnal time-coherent signal and its remainder

baroclinic signal. It suggests $\sum_j P_{df}(\sigma_j)$ is the spectral representation of the spatio-temporal process of internal wave steepening and possibly breaking.

Thus, large scale barotropic $\hat{U}_0$ is found setting a non-linear limit that determines baroclinic $\hat{U}$-length scales, whilst not generating non-linear constituents directly. This can be seen as for $k_0 \rightarrow 0$ barotropic advection yields only forced, non-resonant, dispersive ($\sigma_j = j\sigma$, $k_j = k$) harmonics $\hat{U}_j = (\hat{U}_0/c)^{j-1}\hat{U}/j!$. Using the same γ, these constituents show a much faster energy drop with frequency than the observed σ^{-3} (for $\sigma > M_4$).

Advection of baroclinic M_2, M_4, ..., by motions at other frequencies, such as at the inertial frequency f, leads to spectral amplitudes at M_2+f, M_4+f, ... For areas having approximately the same amplitude at f as $\hat{U}$, the model fits the observations with a γ-value within the above error bounds (see red symbols in Figure 2) with coefficients for q_j that include a frequency correction. As motions at f are supposed to be large-scale they will however not themselves be subject to advection. This implies that there is no spectral route to provide energy at M_2+2f, M_2+3f, ..., or M_4+2f, ..., etc. More seriously, as aluded to above, the combination frequencies M_2+f, M_4+f, ..., loose their spatio-temporal synchronization. Their wave numbers do not increase at the same rate as the combination frequencies, implying a loss of coherence. This reasoning equally applies to motions at all neighbouring frequencies. In fact, Figure 2 shows that the shape of the primary inertial-semidiurnal f/M_2 band is transposed to the M_2+f/M_4 band via the baroclinic tide following (2), and similarly to higher frequency bands. Hereby, the shape-shrink in frequency is attributable to log-log plotting and the self-similar variance-shrink to (2) that equally affects all frequencies in the primary band. The splitting of energy to neighbouring frequencies is in part due to interactions with the slowly varying stratification background (van Haren, 2016).

4. DISCUSSION

Compared to background energy levels, large variance at tidal and inertial-tidal higher harmonics is observed at the deep site, more than 100 km from the continental slope. It may be questioned whether motions at these higher harmonics are reminiscent of non-linear interactions between and by deformation of internal waves in the ocean. Alternatively, these motions may be the result of effects of sloping underwater topography upon which internal waves break. The associated strong turbulence may reach far into the deep ocean. Observations are lacking of turbulence, but numerical internal tide modelling demonstrates the possibility of multiple interactions at such distances from topography (Pichon et al., 2013). The non-linearity as in observed higher harmonics suggests that turbulence may not be negligible locally.

This is because the observed similarity of semidiurnal particle displacement speed and phase speed, as in hydraulic jumps at the point of overturning, suggests a gradient Richardson number Ri ≈ 1. It also suggests a transition from weak wave-wave interaction to, strong, stratified turbulence (Phillips, 1977; D'Asaro and Lien, 2000). Ri ≈ 1 leads to marginal stability for non-linear three-dimensional flows (Abarbanel et al., 1984). In shallow seas, the associated turbulent diapycnal exchange is found sufficient for nutrient replenishment into the photic zone (van Haren et al., 1999). Here, it is interpreted as saturation of non-linear gradients balanced by mixing parameterized by γ. As $\gamma = \pi L/\lambda$ ($L = 2\hat{U}/\sigma$ denoting particle excursion length), the model results imply horizontal wavelength λ of about 5 km of the fundamental constituents and particle speeds of fundamental constituents of 0.05 m s^{-1} as observed, for both inertial-tidal and tidal higher harmonics. Because γ was found independent of N, this length-scale may be fundamental for baroclinic non-linear transfer via advection. Like in shallow seas, the advection term seems to dominantly generate non-linear deep-ocean motions in the Bay of Biscay.

The simple model used here invites future clarification of a balance between internal wave forcing and diapycnal mixing in more sophisticated non-linear internal wave models. As existing numerical models are generally based on the Garrett and Munk (1972) spectrum considering weakly non-linear interactions in the open ocean only, it is suggested to include internal tide breaking at underwater topography. Promising results have been obtained from saturation model of internal tides over abyssal hills that captures the slow decrease of turbulence over at least 500 m from the seafloor and acknowledges the importance of small topography and internal wave scales (Muller and Bühler, 2009). Such models may be extended to include higher harmonics.

ACKNOWLEDGEMENTS

The assistance of the crew of the R/V Pelagia was greatly enjoyed. The Bay of Biscay Boundary (TripeB; Hendrik van Aken) project was supported by grants from the Netherlands organization for the advancement of scientific research, NWO.

COMPETING INTERESTS

The authors have no competing interests to declare.

AUTHOR AFFILIATIONS

Hans van Haren orcid.org/0000-0001-8041-8121
Royal Netherlands Institute for Sea Research (NIOZ), P.O. Box 59, 1790 AB Den Burg, the Netherlands

Leo Maas orcid.org/0000-0003-1523-7548
Institute for Marine and Atmospheric Research (IMAU), University of Utrecht, P.O. Box 80011, 3508 TA Utrecht, the Netherlands

REFERENCES

Abarbanel, HDI, Holm, DD, Marsden, JE and **Ratiu, T.** 1984. Richardson number criterion for the non-linear stability of three-dimensional stratified flow. *Phys. Rev. Lett*., 52: 2352–2355. DOI: https://doi.org/10.1103/PhysRevLett.52.2352

Bak, P, Tang, C and **Wiesenfeld, K.** 1987. Self-organized criticality: An explanation of the 1/f noise. *Phys. Rev. Lett*., 59: 381–384. DOI: https://doi.org/10.1103/PhysRevLett.59.381

Baker, LE and **Sutherland, BR.** 2020. The evolution of superharmonics excited by internal tides in non-uniform stratification. *J. Fluid Mech*., 891: R1, 1–13. DOI: https://doi.org/10.1017/jfm.2020.188

D'Asaro, M and **Lien, R.** 2000. The wave-turbulence transition for stratified flows. *J. Phys. Oceanogr*., 30: 1669–1678. DOI: https://doi.org/10.1175/1520-0485(2000)030<1669:TWTTFS>2.0.CO;2

Dauxois, T, Joubaud, S, Odier, P and **Venaille, A.** 2018. Instabilities of internal gravity wave beams. *Ann. Rev. Fluid Mech*., 50: 131–156. DOI: https://doi.org/10.1146/annurev-fluid-122316-044539

Diamessis, PJ, Wunsch, S, Delwiche, I and **Richter, MP.** 2014. Nonlinear generation of harmonics through the interaction of an internal wave beam with a model oceanic pycnocline. *Dyn. Atmos. Oc*., 66: 110–137. DOI: https://doi.org/10.1016/j.dynatmoce.2014.02.003

Dronkers, JJ. 1964. *Tidal Computations in Rivers and Coastal Waters*. Amsterdam, NL: North Holland Publishing Company, 518 pp.

Eden, C, Pollmann, F and **Olbers, D.** 2019. Numerical evaluation of energy transfers in internal gravity wave spectra of the ocean. *J. Phys. Oceanogr*., 49: 737–749. DOI: https://doi.org/10.1175/JPO-D-18-0075.1

Fan, B and **Akylas, TR.** 2021. Instabilities of finite-width internal wave beams: from Floquet analysis to PSI. *J. Fluid Mech*., 913: A5. DOI: https://doi.org/10.1017/jfm.2020.1172

Garrett, CJR and **Munk, WH.** 1972. Space-time scales of internal waves. *Geophys. Fluid Dyn*., 3: 225–264. DOI: https://doi.org/10.1080/03091927208236082

Groen, P. 1967. On the residual transport of suspended matter by an alternating tidal current. *Neth. J. Sea Res*., 3: 564–574. DOI: https://doi.org/10.1016/0077-7579(67)90004-X

Lamb, KG. 2004. Nonlinear interaction among internal wave beams generated by tidal flow over supercritical topography. *Geophys. Res. Lett*., 31: L09313. DOI: https://doi.org/10.1029/2003GL019393

LeBlond, PH and **Mysak, LA.** 1978. *Waves in the Ocean*, 602. New York, USA: Elsevier.

Lvov, YV, Polzin, KL and **Yokoyama, N.** 2012. Resonant and near-resonant internal wave interactions. *J. Phys. Oceanogr*., 42: 669–691. DOI: https://doi.org/10.1175/2011JPO4129.1

McComas, CH and **Bretherton, FP.** 1977. Resonant interaction of oceanic internal waves. *J. Geophys. Res*., 82: 1397–1412. DOI: https://doi.org/10.1029/JC082i009p01397

Mihaly, SF, Thomson, RE and **Rabinovich, AB.** 1998. Evidence for non-linear interaction between internal waves of inertial and semidiurnal frequency. *Geophys. Res. Lett*., 25: 1205–1208. DOI: https://doi.org/10.1029/98GL00722

Muller, CJ and **Bühler, O.** 2009. Saturation of the internal tides and induced mixing in the abyssal ocean. *J. Phys. Oceanogr*., 39: 2077–2096. DOI: https://doi.org/10.1175/2009JPO4141.1

Müller, P and **Briscoe, M.** 1999. Diapycnal mixing and internal waves. In: *Dynamics of oceanic internal gravity waves, II. Proceedings 'Aha Huliko'a Hawaiian Winter Workshop* (ed. P. Müller and D. Henderson), Hawaii, USA: SOEST, 289–294.

Parker, BB. (ed.) 1991. *Tidal hydrodynamics*. New York, USA: John Wiley & Sons, 883 pp.

Phillips, OM. 1977. *The Dynamics of the upper Ocean* (2nd Ed.). Cambridge, UK: Cambridge University Press, 336 pp.

Pichon, C, Morel, Y, Baraille, R and **Quaresma, LS.** 2013. Internal tide interactions in the Bay of Biscay: Observations and modelling. *J. Mar. Sys*., 109–110: S26–S44. DOI: https://doi.org/10.1016/j.jmarsys.2011.07.003

Pingree, RD and **Maddock, L.** 1978. The M_4 tide in the English Channel derived from a non-linear numerical model of the M_2 tide. *Deep-Sea Res*., 26: 53–68. DOI: https://doi.org/10.1016/S0146-6291(21)00006-0

Pinkel, R, Plueddemann, A and **Williams, R.** 1987. Internal wave observations from FLIP in MILDEX. *J. Phys. Oceanogr*., 17: 1737–1757. DOI: https://doi.org/10.1175/1520-0485(1987)017<1737:IWOFFI>2.0.CO;2

Platzman, GW. 1964. An exact integral of complete spectral equations for unsteady one-dimensional flow. *Tellus*, 16: 422–431. DOI: https://doi.org/10.3402/tellusa.v16i4.8995

Schroeder, M. 1991. *Fractals, chaos, power laws*. New York, USA: W.H. Freeman & Co., 429 pp.

Shrira, VI. 1981. On the propagation of a three-dimensional packet of weakly non-linear internal gravity waves. *Int. J. Non-lin. Mech*., 16: 129–138. DOI: https://doi.org/10.1016/0020-7462(81)90004-4

Thorpe, SA. 1999. On internal wave groups. *J. Phys. Oceanogr*., 29: 1085–1095. DOI: https://doi.org/10.1175/1520-0485(1999)029<1085:OIWG>2.0.CO;2

van Haren, H. 2006. Non-linear motions at the internal tide source. *Geophys. Res. Lett*., 33: L11605. DOI: https://doi.org/10.1029/2006GL025851

van Haren, H. 2016. Do deep-ocean kinetic energy spectra represent deterministic or stochastic signals?

J. Geophys. Res., 121: 240–251. DOI: https://doi.org/10.1002/2015JC011204

van Haren, H and **Gostiaux, L.** 2009. High-resolution open-ocean temperature spectra. *J. Geophys. Res*., 114: C05005. DOI: https://doi.org/10.1029/2008JC004967

van Haren, H, Maas, L and **van Aken, H.** 2002. On the nature of internal wave spectra near a continental slope. *Geophys. Res. Lett*., 29(12). DOI: https://doi.org/10.1029/2001GL014341

van Haren, H, Maas, L, Zimmerman, JTF, Ridderinkhof, H and **Malschaert, H.** 1999. Strong inertial currents and marginal internal wave stability in the central North Sea. *Geophys. Res. Lett*., 26: 2993–2996. DOI: https://doi.org/10.1029/1999GL002352

van Haren, H, Maas, LRM and **Gerkema, T.** 2010. Patchiness in internal tidal beams. *J. Mar. Res*., 68: 237–257. DOI: https://doi.org/10.1357/002224010793721451

Wunsch, C. 1975. Internal tides in the ocean. *Rev. Geophys*. 13: 167–182. DOI: https://doi.org/10.1029/RG013i001p00167

Xing, J and **Davies, AM.** 2002. Processes influencing the non-linear interaction between inertial oscillations, near inertial internal waves and internal tides. *Geophys. Res. Lett*., 29(5). DOI: https://doi.org/10.1029/2001GL014199

TO CITE THIS ARTICLE:
van Haren, H and Maas, L. 2022. A Simple Model for an Internal Wave Spectrum Dominated by Non-Linear Interactions. *Tellus A: Dynamic Meteorology and Oceanography*, 74(1): 382–390. DOI: https://doi.org/10.16993/tellusa.45

Submitted: 28 February 2022 **Accepted:** 14 October 2022 **Published:** 31 October 2022